Kinetochore-microtubule stability governs the metaphase requirement for Eg5

A. Sophia Gayek and Ryoma Ohi
Department of Cell and Developmental Biology, Vanderbilt University Medical Center, Nashville, TN 37232

ABSTRACT **The mitotic spindle is a bipolar, microtubule (MT)-based cellular machine that segregates the duplicated genome into two daughter cells. The kinesin-5 Eg5 establishes the bipolar geometry of the mitotic spindle, but previous work in mammalian cells suggested that this motor is unimportant for the maintenance of spindle bipolarity. Although it is known that Kif15, a second mitotic kinesin, enforces spindle bipolarity in the absence of Eg5, how Kif15 functions in this capacity and/or whether other biochemical or physical properties of the spindle promote its bipolarity have been poorly studied. Here we report that not all human cell lines can efficiently maintain bipolarity without Eg5, despite their expressing Kif15. We show that the stability of chromosome-attached kinetochore-MTs (K-MTs) is important for bipolar spindle maintenance without Eg5. Cells that efficiently maintain bipolar spindles without Eg5 have more stable K-MTs than those that collapse without Eg5. Consistent with this observation, artificial destabilization of K-MTs promotes spindle collapse without Eg5, whereas stabilizing K-MTs improves bipolar spindle maintenance without Eg5. Our findings suggest that either rapid K-MT turnover pulls poles inward or slow K-MT turnover allows for greater resistance to inward-directed forces.**

Monitoring Editor
Kerry S. Bloom
University of North Carolina

Received: Mar 3, 2014
Revised: Apr 28, 2014
Accepted: May 1, 2014

INTRODUCTION

The mitotic spindle is a bipolar, microtubule (MT)-based machine that divides a replicated set of chromosomes into two daughter cells. The spindle consists of stable chromosome-bound kinetochore-MTs (K-MTs), which attach end-on at kinetochores, and short-lived interpolar non–K-MTs, whose plus ends undergo dynamic instability. The bipolar geometry of the spindle is established during prophase by kinesin-5 motors (Sawin *et al.*, 1992; Blangy *et al.*, 1995), which slide antiparallel interpolar MTs apart (Kapitein *et al.*, 2005). The vertebrate kinesin-5, Eg5, is counteracted by the oppositely directed motors dynein and kinesin-14 such that the metaphase spindle reaches a force balance to maintain a steady-state length (Sharp *et al.*, 1999; Mitchison *et al.*, 2005; Tanenbaum *et al.*, 2008). In addition to these motor-generated forces, forces produced by K-MTs become relevant as the K-MTs mature during prometaphase and metaphase (McEwen *et al.*, 1997). It has been suggested that K-MTs generate outward forces that promote spindle assembly (Toso *et al.*, 2009). In addition, K-MTs are believed to generate inward forces through depolymerization (Goshima *et al.*, 2005). The context and extent to which K-MTs generate force in the metaphase spindle are largely unexplored and are complicated by the fact that they coexist with other inward and outward force generators.

Although Eg5 is indisputably important during spindle formation, its role at metaphase varies by cell type. Eg5 is required to maintain spindle bipolarity in *Xenopus* meiotic spindles (Kapoor *et al.*, 2000), where it has been suggested to act as a static crosslinker, perhaps stabilizing parallel oriented MTs near the spindle poles where it concentrates (Uteng *et al.*, 2008). In contrast to meiotic systems, Eg5 is reported to be of limited importance in maintaining spindle bipolarity in human somatic cells (Blangy *et al.*, 1995; Kollu *et al.*, 2009; Tanenbaum *et al.*, 2009; Vanneste *et al.*, 2009). After Eg5 inhibition, maintenance of bipolarity in cultured human cells depends on a second kinesin, the kinesin-12 Kif15 (Tanenbaum *et al.*, 2009; Vanneste *et al.*, 2009), and to a lesser degree on the dynamics of non–K-MTs (Kollu *et al.*, 2009). How Kif15 prevents spindle collapse in the absence of Eg5 is not known. Because kinesin-12s are plus end–directed motors (Boleti *et al.*, 1996), one hypothesis is that Kif15 acts similarly to Eg5, sliding antiparallel MTs

This article was published online ahead of print in MBoC in Press (http://www.molbiolcell.org/cgi/doi/10.1091/mbc.E14-03-0785) on May 7, 2014.

Address correspondence to: Ryoma Ohi (ryoma.ohi@vanderbilt.edu).

Abbreviations used: HURP, hepatoma up-regulated protein; K-MT, kinetochore-microtubule; MT, microtubule; STLC, *S*-trityl-L-cysteine.

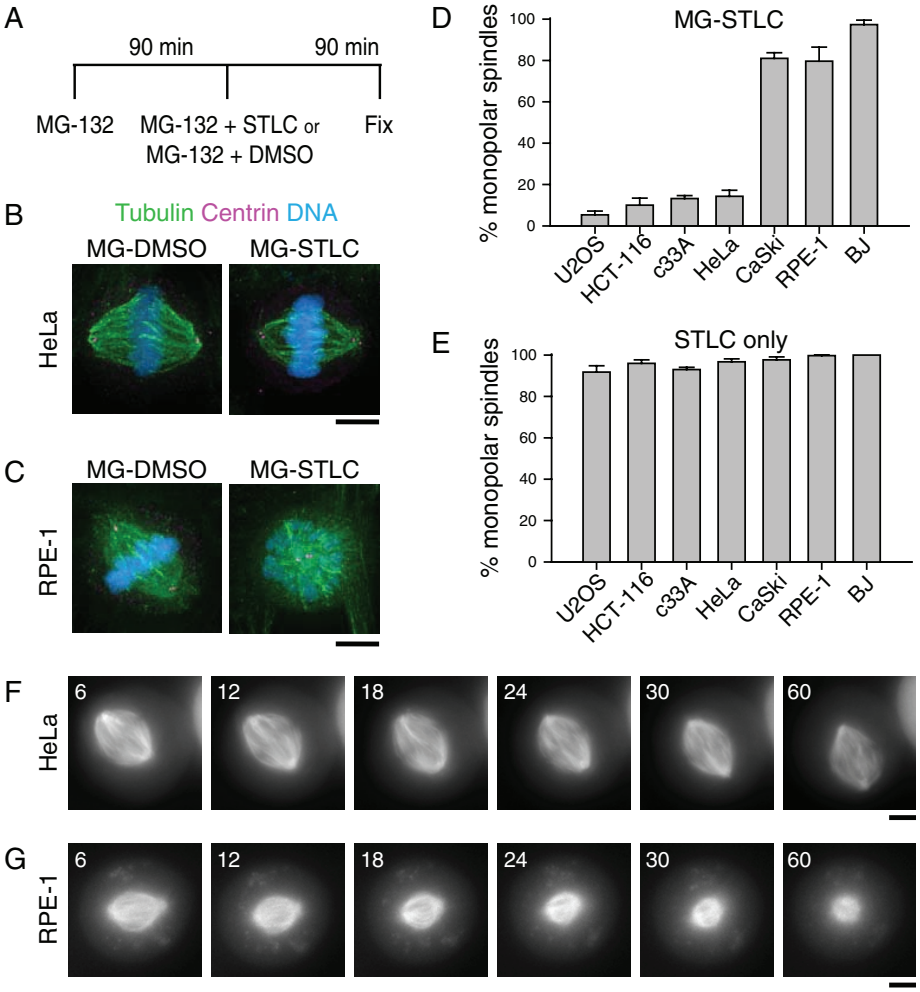

FIGURE 1: The ability of human cell lines to maintain spindle bipolarity in the absence of Eg5 activity varies. (A) Bipolar spindle collapse assay. Cells were arrested in mitosis for 90 min with 5 μM MG-132 and then treated for an additional 90 min with 5 μM MG-132 plus 10 μM STLC to inhibit Eg5 ("MG-STLC") or with 5 μM MG-132 plus DMSO equal in volume to STLC ("MG-DMSO"), and fixed. (B, C) Representative images of HeLa (B) or RPE-1 (C) cells treated with MG-DMSO or MG-STLC. Tubulin (green) and centrin (magenta) were detected by immunostaining. DNA (blue) was counterstained with Hoechst 33342. Scale bar, 5 μm. (D) Quantification of spindle geometries after MG-STLC treatment as described in A. Data represent the mean ± SEM; $n \geq 300$ cells from three experiments. (E) Quantification of spindle geometries after treatment with 10 μM STLC for 90 min without MG-132 treatment. Data represent the mean ± SEM; $n \geq 280$ cells from three experiments. (F, G) Live imaging of HeLa and RPE-1 cell responses to STLC. Still images of HeLa (F) or RPE-1 (G) cells expressing mCherry-tubulin, arrested with 5 μM MG-132 for 100 min, and then treated with 5 μM MG-132 and 10 μM STLC. Time is indicated in minutes and is relative to STLC addition. Scale bar, 5 μm.

apart (Tanenbaum *et al.*, 2009; Tanenbaum and Medema, 2010). However, because Kif15 partitions specifically to parallel-bundled K-MTs (Sturgill and Ohi, 2013), it is likely that it influences spindle bipolarity through a mechanism different from the antiparallel sliding generated by Eg5.

A hallmark of K-MTs is their heightened stability relative to non–K-MTs. Non–K-MTs are short lived, exhibiting half-lives of ~20 s; K-MTs, in contrast, are stable, with half-lives of >180 s (Bakhoum *et al.*, 2009). K-MT half-lives vary widely across human cell lines and are generally longer lived in tumor-derived cells (Bakhoum *et al.*, 2009). For example, K-MTs in U118 glioblastoma cells exhibit a half-life of ~720 s, approximately threefold higher than K-MTs in nontransformed RPE-1 cells (Bakhoum *et al.*, 2009). The increased stability of K-MTs in cancer cells causes frequent mistakes in chromosome segregation (Bakhoum *et al.*, 2009), but, remarkably, does not grossly alter the steady-state size or shape of the mitotic spindle. Given that MTs are rigid polymers (Dogterom and Yurke, 1997), it is reasonable to expect that the long-lived K-MTs in cancer cells might also change physical properties of the metaphase spindle, yet such changes have not been identified.

Here we report that in contrast to most cancer cells, nontransformed human cells require Eg5 to maintain spindle bipolarity. We find that the metaphase dependence on Eg5 correlates with low K-MT stability and that experimental alteration of K-MT stability predictably affects the ability of cells to maintain spindle bipolarity without Eg5. Our findings suggest that long-lived K-MTs enforce spindle bipolarity, either by reducing K-MT pulling forces or by increasing the mechanical robustness of the metaphase spindle.

RESULTS

Eg5 is essential for robust maintenance of spindle bipolarity in some cell types

To determine whether Eg5 is universally dispensable for maintaining spindle bipolarity in human cells, we used an assay (Tanenbaum *et al.*, 2009) that tests the ability of metaphase cells to maintain spindle bipolarity upon exposure to *S*-trityl-L-cysteine (STLC), a small-molecule inhibitor of Eg5 (DeBonis *et al.*, 2004). Briefly, we treated a panel of human cell lines with the proteasome inhibitor MG-132 for 90 min to allow for bipolar spindle assembly and then treated the cells with MG-132 and STLC for a further 90 min (Figure 1A; MG-STLC). An identical treatment using dimethyl sulfoxide (DMSO) in place of STLC was used as a vehicle control (Figure 1A; MG-DMSO). A 90-min treatment with MG-132 causes accumulation of mitotic cells at metaphase by blocking cyclin B degradation, so STLC application chiefly affects bipolar spindle maintenance rather than bipolar spindle formation.

We found that human cell lines have different capacities to maintain spindle bipolarity in the absence of Eg5 activity. In accordance with prior reports (Blangy *et al.*, 1995; Kollu *et al.*, 2009; Tanenbaum *et al.*, 2009), most spindles were bipolar after MG-STLC treatment in HeLa (84.3 ± 2.3%, mean ± SEM; n = 300), U2OS (94.0 ± 1.5%; n = 300), HCT116 (89.0 ± 3.4%; n = 300), and c33A cells (86.0 ± 1.2%; n = 400; Figure 1, B and D). Unexpectedly, most spindles were monopolar after the same drug treatments in RPE-1 (79.7 ± 6.8%; n = 300), BJ (97.3 ± 2.2%; n = 300), and CaSki cells (81.0 ± 2.7%; n = 400; Figure 1, C and D), suggesting that Eg5 is necessary for efficient bipolar spindle maintenance in these cell lines. Of importance, resistance to STLC cannot explain this cell line variability. In all cell lines, >90% of mitotic cells contained monopolar spindles when

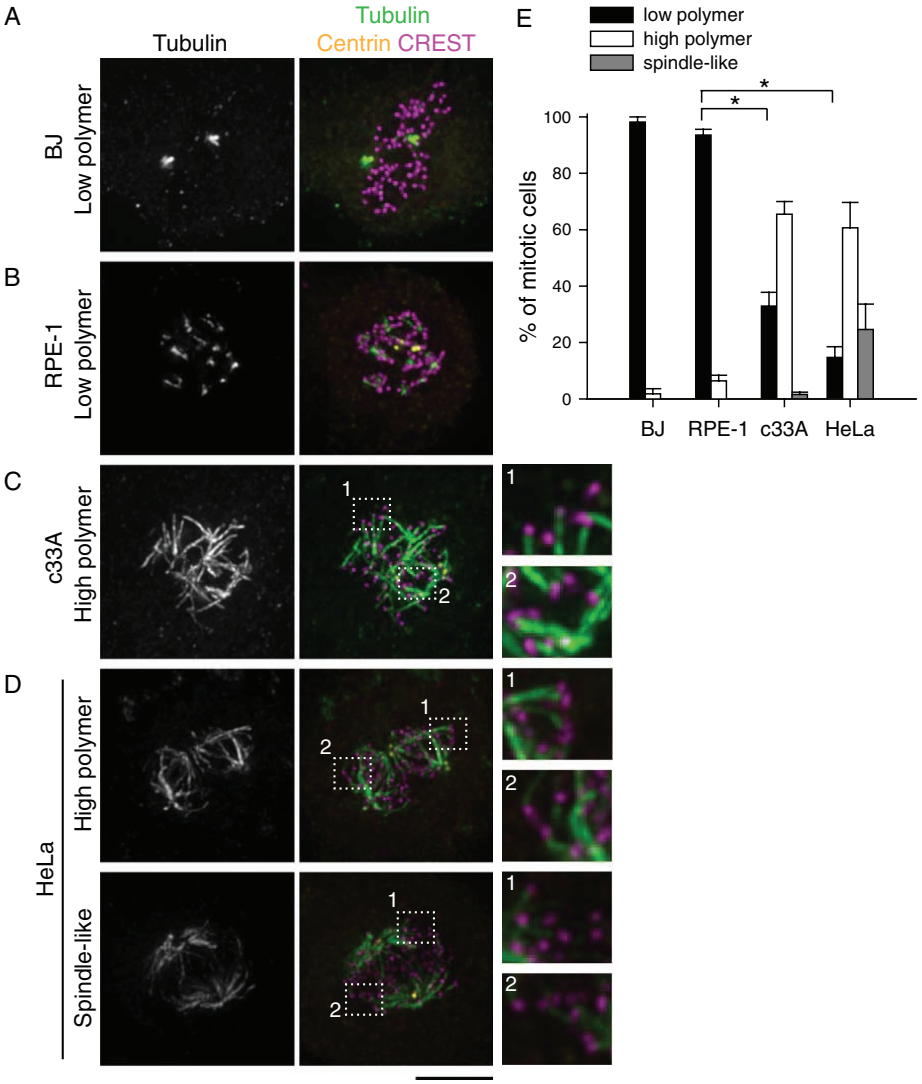

FIGURE 2: High K-MT stability correlates with efficient bipolar spindle maintenance without Eg5. (A–D) Images of BJ (A), RPE-1 (B), c33A (C), and HeLa (D) cells that were arrested in mitosis with 5 µM MG-132 for 90 min and then treated with 5 µM nocodazole for 6 min, extracted for 20 s, and fixed. Tubulin (green), centrin (yellow), and kinetochores (magenta; CREST) were detected by immunostaining. DNA (blue) was counterstained with Hoechst 33342. Dotted line shows region enlarged threefold. Scale bar, 5 µm. A and C are from a single experiment, and B and D are from a single experiment. Lookup tables (LUTs) were adjusted identically for images corresponding to the same experiment. (E) Quantification of residual MT polymer levels after nocodazole treatment. Puncta or short streaks were scored as "low polymer," and long streaks joined at nodes were scored as "high polymer"; long streaks joined in two poles were scored as "spindle-like." Data represent the mean ± SEM; $n \geq 100$ cells from at least three experiments. *$p < 0.001$.

treated with STLC for 90 min without MG-132 ($n \geq 280$; Figure 1E), demonstrating that they were susceptible to the drug. In addition, STLC displaced Eg5 from the spindle in cell lines that collapsed, as well as in those that maintained bipolarity without Eg5 (Supplemental Figure S1), further demonstrating susceptibility to the drug.

To verify that a high prevalence of monopolar spindles after MG-STLC treatment stemmed from bipolar spindle collapse rather than a failure to establish bipolarity, we monitored the STLC response of preassembled bipolar spindles by live-cell imaging of fluorescent tubulin. After an MG-132 arrest and STLC treatment, bipolar spindles collapsed to monopoles in 17 of 31 RPE-1 cells within 1 h after STLC application (55%; Figure 1G); this may be lower than the percentage of monopoles in fixed-cell assays because a small number of cells may enter mitosis during incubation with STLC. In contrast to RPE-1 cells, a bipolar spindle collapsed to a monopole in only 1 of 25 HeLa cells in the same time window (4%; Figure 1F). These results demonstrate that although Eg5 is required for the formation of bipolar spindles in all cell lines tested, it is dispensable for the maintenance of bipolar spindles in some but not all cell lines.

High K-MT stability correlates with bipolar spindle maintenance without Eg5

To understand the different abilities of human cell lines to maintain spindle bipolarity in the absence of Eg5 activity, we considered Kif15, the motor protein most necessary for bipolar spindle maintenance without Eg5 in HeLa and U2OS cells (Tanenbaum *et al.*, 2009; Vanneste *et al.*, 2009; Sturgill and Ohi, 2013). Kif15 is expressed and localizes to the mitotic spindle in RPE-1 cells, suggesting that a lack of Kif15 cannot explain the sensitivity of RPE-1 cells to STLC at metaphase (Supplemental Figure S2). Of interest, Kif15 localizes specifically to K-MTs (Sturgill and Ohi, 2013), which are required for spindle bipolarity without Eg5 (Sturgill and Ohi, 2013). In addition, K-MT stability is known to vary among human cell lines. Nontransformed cell lines, including RPE-1, have less-stable K-MTs than transformed cell lines, including U2OS (Bakhoum *et al.*, 2009). Because Kif15 localizes to K-MTs and K-MT stability is known to vary among human cell lines, we asked whether K-MT stability can explain the differences in the abilities of cell lines to maintain bipolarity without Eg5.

To assess the stability of K-MTs, we developed an assay using the tubulin-sequestering drug nocodazole. In cells treated with nocodazole for short time periods (a "nocodazole shock"), MTs that turn over rapidly disappear, but MTs that turn over slowly persist. We used nocodazole shock rather than fluorescence dissipation following photoactivation (FDAP; Zhai *et al.*, 1995; Bakhoum *et al.*, 2009; Kabeche and Compton, 2013) for three reasons. First, although nocodazole shock does not report quantitative information on K-MT half-lives, it does provide enough temporal resolution to see reproducible differences across cell lines (Figure 2E). Furthermore, nocodazole shock allows for the rapid analysis of higher numbers of cells than FDAP. Finally, counterstaining of kinetochores allows us to verify that the nocodazole-resistant polymer we see is derived from K-MTs instead of non-kinetochore-MTs (Figure 2, C and D), information that FDAP cannot provide. We verified that nocodazole shock gives similar results to a well-established method by monitoring cold-stable MT levels. The K-MT stability trend revealed by cold temperatures (Supplemental Figure S3)

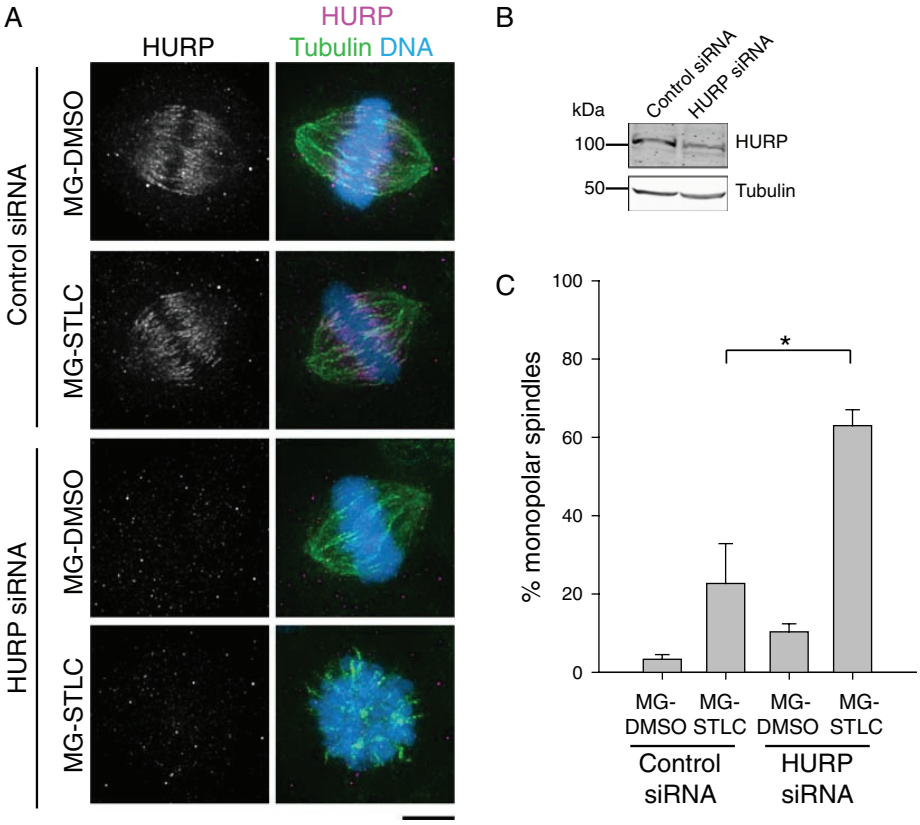

FIGURE 3: Depletion of HURP undermines bipolar spindle maintenance in HeLa cells after Eg5 inhibition. (A) HURP depletion renders bipolar spindles in HeLa cells sensitive to Eg5 inhibition. HeLa cells transfected with control or HURP siRNA were treated with MG-DMSO or MG-STLC. Representative spindle geometries are shown. LUTs were scaled identically. Scale bar, 5 μm. (B) Immunoblots of cell extracts prepared from cells depleted of HURP by siRNA transfection. To increase HURP signal, both control and HURP siRNA cells were treated with 5 μM MG-132 for 5 h before lysis. Tubulin is shown as a loading control. (C) Quantification of HeLa spindle geometries after treatment as in A. Data represent the mean ± SEM; $n \geq 300$ cells from three experiments. *$p < 0.05$.

matched the trend from nocodazole shock (Figure 2, B, D, and E). We continued with nocodazole shock because nocodazole is well characterized as a MT-specific agent, whereas prolonged cold temperatures are likely to affect other cellular processes.

In accordance with published results (Bakhoum *et al.*, 2009), we found that K-MTs in RPE-1 and BJ cells are unstable compared with those in HeLa or c33A cells (Figure 2). After a 6-min treatment with 5 μM nocodazole, nearly all RPE-1 and BJ cells had low levels of MT polymer (puncta or short MTs only; $n \geq 100$; Figure 2, A and B). In contrast, most HeLa and c33A cells had high levels of polymer; indeed, some cells retained a spindle-like structure with abundant K-MTs ($n \geq 100$; Figure 2, C and D). Therefore, among these four cell lines, the ability to efficiently maintain bipolarity without Eg5 correlates with high K-MT stability, consistent with the idea that K-MT stability affects bipolar spindle maintenance without Eg5.

Destabilizing K-MTs undermines bipolar spindle maintenance in HeLa cells

The model in which cells with more stable K-MTs are better able to maintain bipolarity without Eg5 at metaphase makes two predictions: 1) destabilizing K-MTs would impair bipolar spindle maintenance, and 2) stabilizing K-MTs would promote bipolar spindle maintenance. To test the first prediction, we destabilized K-MTs in HeLa cells by depleting either of two K-MT stabilizing factors, hepatoma up-regulated protein (HURP) or astrin (Figures 3B and 4B; Sillje *et al.*, 2006; Manning *et al.*, 2010). Transfection of siRNAs targeting either HURP or astrin decreased K-MT stability as gauged by the nocodazole shock assay (Supplemental Figures S4 and S5). Cells transfected in the same way were treated with MG-132 and STLC as in Figure 1A. Depletion of HURP did not significantly alter spindle geometries in cells treated with MG-132 and DMSO (Figure 3, A and C). However, depletion of HURP and inhibition of Eg5 with STLC produced a strong increase in monopolar spindles (63.0 ± 4.0%; $n = 300$) compared with control siRNA cells (10.3 ± 2.0%; $n = 300$; Figure 3, A and C). This result supports the idea that high K-MT stability is necessary for bipolar spindle maintenance without Eg5.

As previously reported (Thein *et al.*, 2007; Manning *et al.*, 2010), depletion of astrin caused an increase in multipolar spindles (65.7 ± 4.7%; $n = 300$) compared with control siRNA cells (2.0 ± 1.0%; $n = 300$; Figure 4, A and C) in cells not treated with STLC. However, depletion of astrin caused a strong increase in monopolar spindles after MG-STLC treatment (73.0 ± 4.2%; $n = 300$) compared with control siRNA cells (15.6 ± 3.3%; $n = 300$; Figure 4, A and C), in accordance with our results on HURP depletion. To test whether the multipolar spindles produced by astrin depletion are predisposed to collapse to monopolar spindles without Eg5, we generated multipolar spindles by a different method and monitored their response to STLC treatment after an MG-132 arrest. We blocked cytokinesis in HeLa cells with the actin poison cytochalasin B, doubling both DNA content and centrosome number (Figure 4D). This treatment increased multipolar spindles without STLC but did not increase the prevalence of monopolar spindles in cells treated with STLC relative to cells not treated with cytochalasin B (Figure 4, D and E). This result suggests that in HeLa cells depleted of astrin, it is the reduction of K-MT stability, not the generation of multipolar spindles, that drives the collapse to monopolar spindles without Eg5.

Stabilization of K-MTs promotes bipolar spindle maintenance without Eg5 in RPE-1 cells

To test the second prediction, we stabilized MTs in RPE-1 cells using a low concentration of Taxol (2.5 nM). Taxol was applied at the start of the MG-132 arrest and was present through the STLC challenge (Figure 1A). At 2.5 nM, Taxol did not cause gross changes in spindle geometry in DMSO-treated cells, but it strongly reduced the number of monopolar spindles after MG-STLC (23.9 ± 6.2%; $n = 355$) compared with non–Taxol-treated cells (95.8 ± 2.0%; $n = 330$; Figure 5, A and B). We confirmed this finding in live cells by filming fluorescent tubulin. Spindles in 23 of 25 MG-132-arrested RPE-1 cells treated with 2.5 nM Taxol remained bipolar after 1 h of STLC treatment (92%; Figure 5D). Of importance, the MT stability increase conferred by 2.5 nM Taxol did not strongly interfere with mitotic progression. Differential interference contrast microscopy of RPE-1

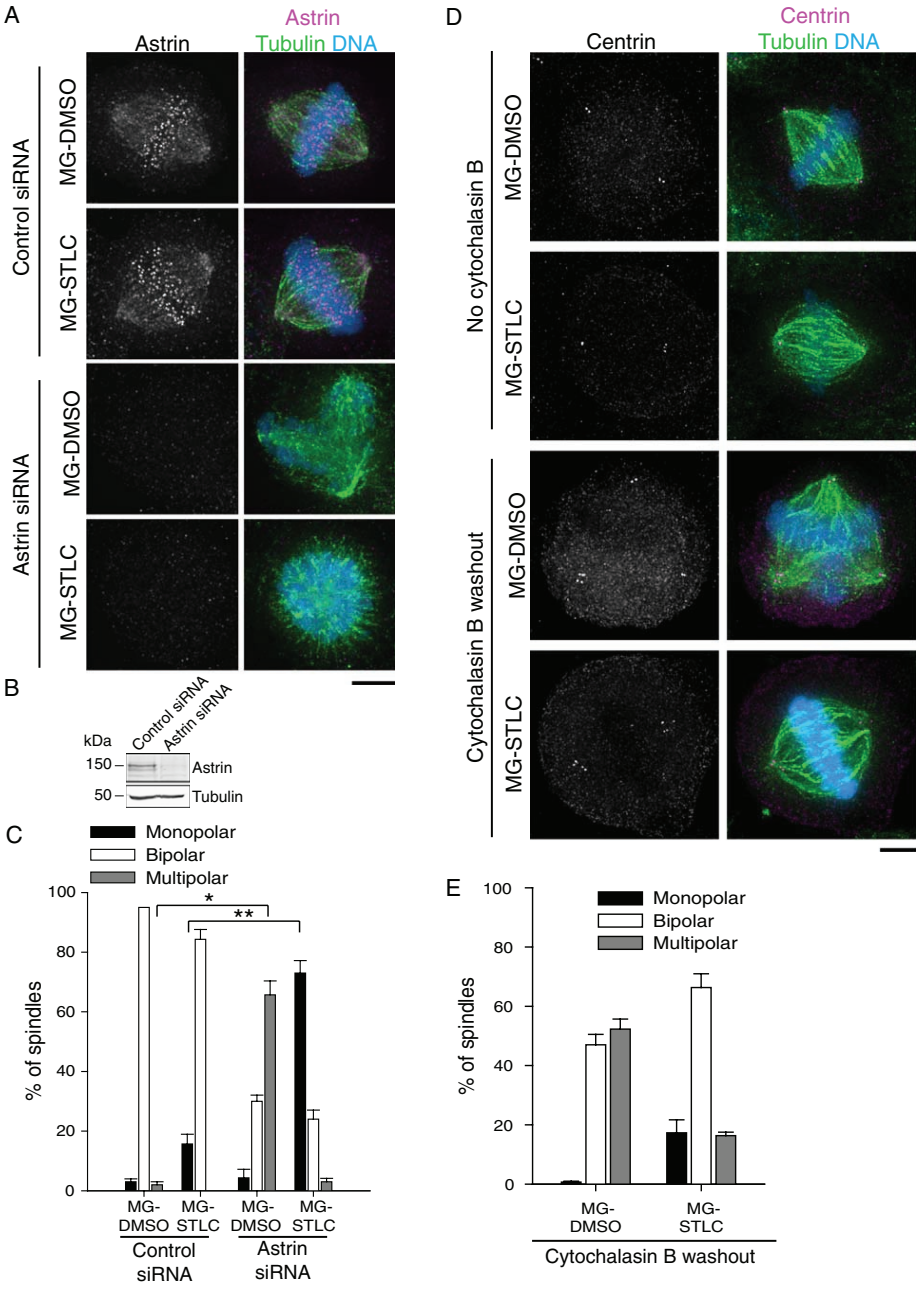

FIGURE 4: Depletion of astrin undermines bipolar spindle maintenance in HeLa cells after Eg5 inhibition. (A) Astrin depletion renders bipolar spindles in HeLa cells sensitive to Eg5 inhibition. HeLa cells transfected with control or astrin siRNA were treated with MG-DMSO or MG-STLC. Representative spindle geometries are shown. LUTs were scaled identically. Scale bar, 5 µm. (B) Immunoblots of cell extracts prepared from cells depleted of astrin by siRNA transfection. Tubulin is shown as a loading control. (C) Quantification of HeLa spindle geometries after treatment as in A. Data represent the mean ± SEM; $n \geq 300$ cells from three experiments. *$p < 0.005$; **$p < 0.001$. (D) Spindle multipolarity does not cause sensitivity to Eg5 inhibitors. HeLa cells were incubated in media with or without cytochalasin B for 24 h. At 18 h after cytochalasin B washout, cells were treated with MG-DMSO or MG-STLC as in Figure 1A. Representative images show centrosome duplication and resulting spindle geometries. LUTs were scaled identically. Scale bar, 5 µm. (E) Quantification of HeLa spindle geometries after treatment as in D. Data represent the mean ± SEM; $n \geq 300$ cells from three experiments.

cells treated with 2.5 nM Taxol showed that the time from nuclear envelope breakdown to anaphase onset was slightly increased by the drug, but cells were nevertheless able to satisfy the spindle assembly checkpoint and exit mitosis (Figure 5C).

We confirmed that 2.5 nM Taxol increased K-MT stability using nocodazole shock (Figure 5, E and F). In contrast to untreated RPE-1 cells (Figure 2), RPE-1 cells treated with 2.5 nM Taxol had high polymer levels after nocodazole shock (Figure 5, E and F). To verify that Taxol stabilized bipolarity through K-MTs, we blocked K-MT formation by depleting cells of the outer kinetochore component Nuf2 (DeLuca *et al.*, 2002) and treated them with MG-STLC or MG-DMSO in the presence of 2.5 nM Taxol. In accordance with published results (DeLuca *et al.*, 2002), Nuf2 depletion produced bipolar spindles with a banana-shaped morphology and misaligned chromosomes (Figure 5G). Such cells were unable to maintain bipolarity with 2.5 nM Taxol (96.2 ± 1.5% monopolar; $n = 104$; Figure 5, G and H), suggesting that stabilizing non–K-MTs is not sufficient to maintain bipolarity. This demonstrates that artificially increasing K-MT stability in RPE-1 cells enhances their ability to maintain spindle bipolarity without Eg5.

Perturbing K-MT stability influences bipolar spindle maintenance independently of Kif15 levels

Because Kif15 fails to bind the spindle in HeLa cells without K-MTs (Sturgill and Ohi, 2013), it is possible that our K-MT stability perturbations affect bipolar spindle maintenance by affecting Kif15 levels rather than by having a direct effect on K-MT–generated forces. To examine this, we measured spindle-bound Kif15 fluorescence in HeLa cells depleted of HURP (Figure 6, A and B) and in RPE-1 cells treated with 2.5 nM Taxol (Figure 6, C and D). Although each of these perturbations affects the ability of cells to maintain spindle bipolarity without Eg5, neither perturbation changed the binding of Kif15 to the spindle. We therefore conclude that modulation of K-MT stability acts independently of Kif15 localization.

DISCUSSION

Force balance, in which sliding forces generated by molecular motors are coupled to MT depolymerization, has provided a useful framework for understanding length control of the metaphase spindle (Goshima *et al.*, 2005). Kinesin-5 motors are central to this model, and it has been argued that they act continuously throughout metaphase to antagonize inward-directed forces generated by depolymerization of K-MTs (Goshima *et al.*, 2005) or motors of opposite directionality (Tanenbaum *et al.*, 2008). However, Eg5 is not required for bipolarity at metaphase in some vertebrate cell lines (Kollu *et al.*, 2009; Tanenbaum *et al.*, 2009; Vanneste *et al.*, 2009), indicating that other mechanisms must

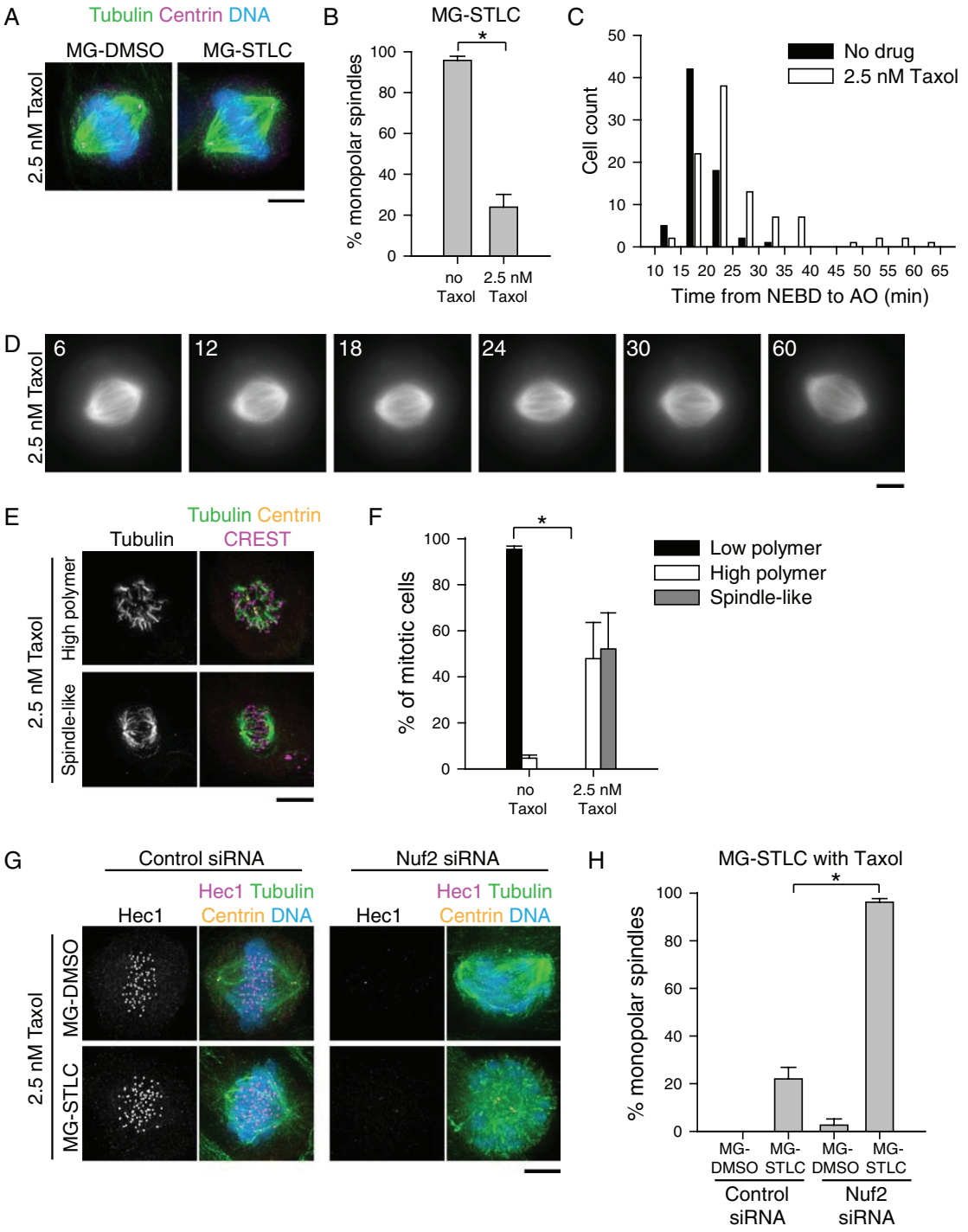

FIGURE 5: Stabilization of K-MTs improves bipolar spindle maintenance in RPE-1 cells after Eg5 inhibition. (A) Low concentrations of Taxol prevent spindle collapse in RPE-1 cells exposed to STLC. Representative images of RPE-1 cells treated with 2.5 nM Taxol plus MG-DMSO or MG-STLC as in Figure 1A. Tubulin (green) and centrin (magenta) were detected by immunostaining. DNA (blue) was counterstained with Hoechst 33342. LUTs were scaled identically. Scale bar, 5 μm. (B) Quantification of spindle geometries after MG-STLC treatment in RPE-1 cells treated with or without 2.5 nM Taxol. Data represent the mean ± SEM; $n \geq 300$ cells from three experiments. *$p < 0.001$. (C) At 2.5 nM, Taxol does not prevent mitotic progression in RPE-1 cells. RPE-1 cells treated with or without 2.5 nM Taxol were filmed by differential interference contrast, and the time from nuclear envelope breakdown (NEBD) to anaphase onset (AO) was quantified. $n \geq 68$ cells from two experiments. (D) Live-cell imaging of an RPE-1 spindle challenged with STLC in the presence of 2.5 nM Taxol. Still images of an RPE-1 cell expressing mCherry-tubulin treated first with 2.5 nM Taxol and 5 μM MG-132 for 100 min and then treated with 2.5 nM Taxol, 5 μM MG-132, and 10 μM STLC. Time is indicated in minutes and is relative to STLC addition. Scale bar, 5 μm. (E) At 2.5 nM, Taxol promotes K-MT survival of nocodazole shock in RPE-1 cells. Representative images of RPE-1 cells treated with nocodazole as in Figure 2 in the presence of 2.5 nM Taxol. Tubulin (green) and centrin (magenta) were detected by immunostaining. DNA (blue) was counterstained

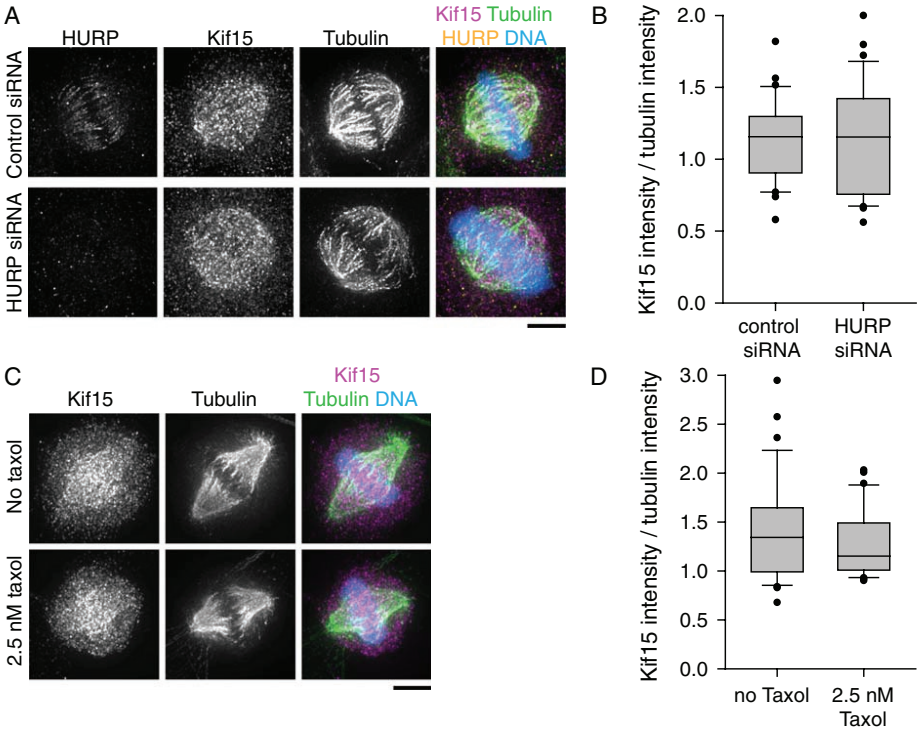

FIGURE 6: Kif15 spindle localization is independent of K-MT stability. (A) Kif15 spindle localization is not reduced in HeLa cells depleted of HURP. HeLa cells transfected with control or HURP siRNA were treated with 5 µM MG-132 for 90 min. HURP (yellow), Kif15 (magenta), and tubulin (green) were detected by immunostaining. DNA (blue) was counterstained with Hoechst 33342. LUTs are scaled identically for each channel. Scale bar, 5 µm. (B) Ratio of spindle Kif15 intensity to spindle tubulin intensity after treatment as in A. Box-and-whisker plots display median flanked by 10th, 25th, 75th, and 90th percentiles. Each data set includes at least 30 cells from three experiments. $p = 0.86$. (C) Kif15 spindle localization is not increased in RPE-1 cells treated with 2.5 nM Taxol. RPE-1 cells were treated with 5 µM MG-132 with or without 2.5 nM Taxol for 90 min. Kif15 (magenta) and tubulin (green) were detected by immunostaining. DNA (blue) was counterstained with Hoechst 33342. LUTs are scaled identically for each channel. Scale bar, 5 µm. (D) Ratio of spindle Kif15 intensity to spindle tubulin intensity after treatment as in C. Box-and-whisker plots display median flanked by 10th, 25th, 75th, and 90th percentiles. Each data set includes at least 30 cells from three experiments. $p = 0.22$.

enforce bipolarity. Our findings highlight the potential importance of K-MTs in bipolarity maintenance. High K-MT stability correlates with the ability to maintain bipolarity without Eg5. Destabilizing K-MTs by depleting HURP or astrin, in contrast, impairs the ability to maintain bipolarity, whereas stabilizing K-MTs with low doses of Taxol has the reverse effect. We note that depletion of HURP or astrin, or treatment with low doses of Taxol, may produce complicated effects beyond merely stabilizing or destabilizing K-MTs; however, the most parsimonious interpretation of our results is that K-MT stability dictates the maintenance of spindle bipolarity without Eg5.

Our findings are consistent with at least two models (Figure 7). First, K-MTs may play an active role in spindle collapse, by which depolymerization of unstable K-MT plus ends generates significant inward-directed forces. In contrast, the plus-end depolymerization of stable K-MTs may not be sufficiently synchronized to generate inward-directed forces. This model is conceptually similar to the model proposed by Ganem and Compton (2004). However, this active, K-MT pulling model does not take into account the fact that spindles lacking K-MTs collapse without Eg5 (Figure 5H; Sturgill and Ohi, 2013), implying the existence of secondary inward-directed forces. Second, K-MTs may play a passive role during spindle maintenance, resisting collapse driven by other inward-directed forces, perhaps generated by minus end–directed motors (i.e., dynein and HSET). Stable K-MTs, organized into a long-lived, tightly packed bundle, would have great flexural rigidity (Felgner *et al.*, 1997) and thus be able to withstand inward forces generated by motors of opposite directionality to Eg5. Of importance, this passive, outward force would be produced only when inward force was applied on the poles; therefore, it would not disrupt the steady-state length of the spindle with Eg5. Future work will be directed at discriminating between these possibilities.

The passive K-MT pushing model predicts that because the enforcement of bipolarity increases with decreasing K-MT turnover rates, it increases as a function of kinetochore occupancy by MTs. Unfortunately, existing methods to examine K-MT dynamics report only on MT turnover (Zhai *et al.*, 1995; Bakhoum *et al.*, 2009), not on how long a single binding site is empty before it is filled by a regrowing MT. The best available readout for unoccupied K-MT binding sites is kinetochore localization of components of the spindle assembly checkpoint. These will not be useful for determining K-MT occupancy times at metaphase, however, because SAC components require multiple empty MT-binding sites at a single kinetochore and several minutes of time before they are detectable (Dick and Gerlich, 2013). A binding site with a net "occupied" state, as K-MT–binding sites are presumed to be at metaphase, will not generate a signal fast or strong enough to be detected. In the future, it will be important to measure the proportion of time a K-MT–binding site is occupied to understand how this timing affects K-MT–generated forces.

In addition to HURP and astrin, other proteins that act predominantly on K-MTs are known to stabilize the metaphase spindle in the absence of Eg5. Loss of Kif18A reduces K-MT stability (Manning *et al.*, 2010) and also renders bipolar spindles sensitive to Eg5 inhibitors (Tanenbaum *et al.*, 2009). These findings are consistent with our model in which K-MT stability governs the requirement for Eg5 at metaphase. The protein factor known to synergize most strongly

with Hoechst 33342. Scale bar, 5 µm. (F) Quantification of residual MT polymer levels of RPE-1 cells with or without 2.5 nM Taxol after nocodazole treatment as in E. Data represent the mean ± SEM; $n \geq 150$ cells from four experiments. *$p < 0.001$. (G) The protective effect of low-dose Taxol on STLC depends on K-MTs. RPE-1 cells transfected with control or Nuf2 siRNA were treated with MG-DMSO or MG-STLC in the presence of 2.5 nM Taxol. Representative spindle geometries are shown. LUTs are scaled identically. Scale bar, 5 µm. (H) Quantification of spindle geometries after treatment as in G. Data represent the mean ± SEM; $n \geq 95$ cells from three experiments. *$p < 0.005$.

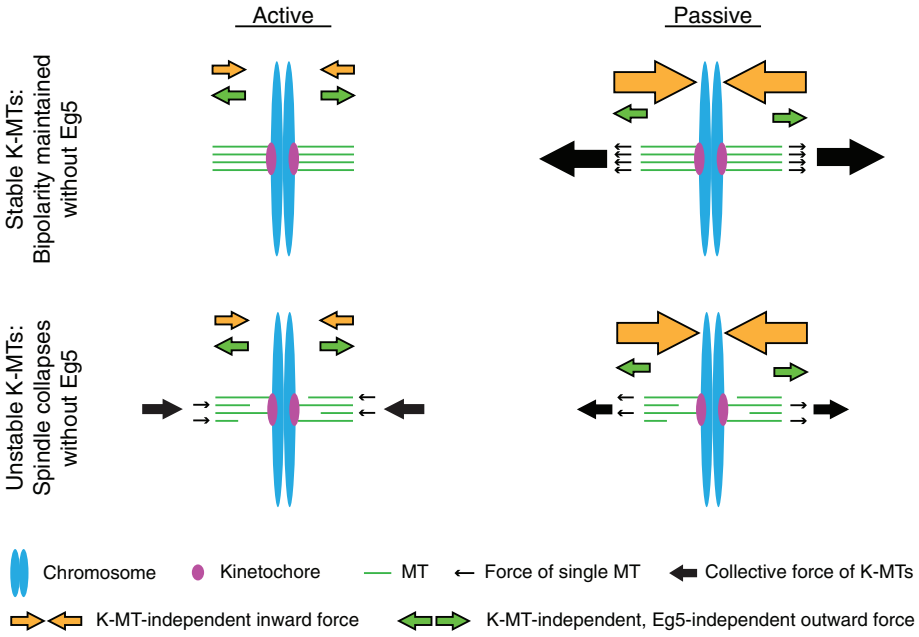

FIGURE 7: Model: K-MT stability determines the relative importance of Eg5 in maintaining spindle bipolarity. Cells with long-lived K-MTs (top) do not continuously require Eg5, either because stable K-MTs do not pull on poles or because stable K-MTs are competent to withstand stronger pulling forces. Cells with short-lived K-MTs (bottom) continuously require Eg5, either because K-MT depolymerization pulls poles inward or because unstable K-MTs cannot withstand pulling forces from other sources.

with Eg5 in enforcing spindle bipolarity is Kif15 (Tanenbaum *et al.*, 2009; Vanneste *et al.*, 2009), a motor that decorates the K-MT lattice (Sturgill and Ohi, 2013; Vladimirou *et al.*, 2013). The biochemical properties of Kif15 central to this activity are not known, but because other K-MT–stabilizing factors enforce bipolar spindle maintenance, our data suggest that the mechanism of Kif15 may also involve stabilization of K-MTs.

Our results suggest that maintenance of bipolarity is derived from spindle properties more complex than a purely motor-driven, push–pull mechanism. The architecture and dynamics of spindle MTs may also be key. Meiotic spindles assembled in *Xenopus* egg extracts, for example, have a low proportion of K-MTs to short-lived non–K-MTs and continuously require Eg5 to maintain bipolarity (Kapoor *et al.*, 2000). However, experimental elevation of the ratio of K-MTs to non–K-MTs causes spindles to become resistant to Eg5 inhibitors (Houghtaling *et al.*, 2009). Even in mitotic human cells, which are constructed from roughly equivalent amounts of non–K-MTs and K-MTs, the requirement for stable K-MTs to maintain bipolarity without Eg5 may not be universal. Although we demonstrated that stable K-MTs promote bipolar spindle maintenance in HeLa and RPE-1 cells, other work suggested that K-MTs are unnecessary for bipolar spindle maintenance without Eg5 in U2OS cells (Kollu *et al.*, 2009). Such phenotypic variation may be due to complex differences in genotype among transformed cells. Indeed, even cell lines with equivalently hyperstable K-MTs have varying levels of key mitotic proteins (Bakhoum *et al.*, 2009). Of importance, however, our study shows that both nontransformed cell lines tested (RPE-1 and BJ) share the same response, suggesting that inefficient bipolar spindle maintenance without Eg5 may be the prevailing phenotype among nontransformed human cells and that bipolar spindle maintenance can be enhanced in these genetically normal cells by stabilizing K-MTs. One implication of our findings is that Eg5 inhibitors should not be used in combination with MT-stabilizing agents such as Taxol, as such treatment regimens may impair rather than improve the killing of tumor cells.

MATERIALS AND METHODS

Cell culture and transfections

All cell lines were grown in media supplemented with 10% fetal bovine serum (FBS) and antibiotics. Medium for RPE-1/mCherry-tubulin stable cells was additionally supplemented with 500 µg/ml G418. HeLa "Kyoto," c33A, HCT116, and BJ-hTERT cells (a gift from David Cortez, Vanderbilt University Medical Center, Nashville, TN) were cultured in DMEM. RPE-1 cells were cultured in 50% DMEM/50% Ham's F-12. U2OS cells were cultured in McCoy's 5A. CaSki cells were cultured in RPMI.

DNA transfections of HeLa and RPE-1 cells were performed using Lipofectamine 2000 (Invitrogen, Carlsbad, CA) or FuGENE 6 (Roche, Indianapolis, IN), respectively, according to the manufacturer's instructions. siRNA transfections were performed with HiPerFect (Qiagen, Valencia, CA) according to the manufacturer's instructions. The following siRNA sequences were used: astrin, TCCCGACAACTCACAGAGAAA (Thein *et al.*, 2007; Qiagen); HURP, CCAGUUACACCUGGACUCCUUUAAA (Ye *et al.*, 2011; Invitrogen); and Nuf2, AAACGAUAGUGCUGCAAGA, GGAUUGCAAUAAAGUUCAA, UAGCUGAGAUUGUGAUUCA, and GAACGAGUAACCACAAUUA (ON-TARGETplus SMARTpool; Thermo Scientific). As negative control, Low GC Duplex or Low GC Duplex#2 scrambled RNA (Invitrogen) was used. Cells were used 48 h (HeLa) or 72 h (RPE-1) after siRNA transfection.

A polyclonal RPE-1 cell line expressing mCherry-tubulin was generated by selecting stably transfected cells with G418, followed by flow cytometry to select for fluorescence-positive cells. Flow cytometry was performed in the Vanderbilt University Medical Center Flow Cytometry Shared Resource (Nashville, TN).

To destabilize MTs, cells were incubated on ice with MG-132 for 29 min or treated with nocodazole for 6 min.

Drugs

Drug stocks in DMSO were stored at −20°C and diluted in media immediately before use. MG-132 (CalBioChem, San Diego, CA) was used at 5 µM for 90 min to 5 h. STLC (Sigma-Aldrich, St. Louis, MO) was used at 10 µM for 90 min. Taxol (Sigma-Aldrich) was used at 2.5 nM for 90–180 min. Nocodazole (Sigma-Aldrich) was used at 5 µM for 6 min. Cytochalasin B (Sigma-Aldrich) was used at 3 µg/ml for 24 h and washed out six times over the course of 30 min; this was adapted from a published method (Yi *et al.*, 2011). All drug treatments were performed at 37°C under culturing conditions.

Generation of centrin antibodies

Centrin 1 (GenBank Accession No. BC084063) was PCR amplified from a *Xenopus laevis* ovary cDNA library (a gift from A. Straight, Stanford University, Stanford, CA) and expressed in BL-21(DE3) cells as a glutathione *S*-transferase (GST) fusion protein. GST-centrin was purified on glutathione agarose (Sigma-Aldrich) and used to immunize rabbits (Cocalico). Centrin-specific antibodies were

affinity purified by passing anti-GST-depleted serum over Affi-Gel 10 (Bio-Rad, Hercules, CA) covalently coupled to GST-centrin. Affinity-purified antibodies were dialyzed into phosphate-buffered saline (PBS), frozen in liquid nitrogen, and stored at –80°C.

Antibodies

The following primary antibodies were also used in this study: mouse anti-tubulin (DM1α; Vanderbilt Antibody and Protein Resource, Nashville, TN); rat anti-tubulin (YL1/2; Accurate Chemical and Scientific Corporation, Westbury, NY); rabbit anti-Eg5 (Miyamoto *et al.*, 2004); rabbit anti-Kif15 (Sturgill and Ohi, 2013); rabbit anti-astrin (Santa Cruz Biotechnology, Dallas, TX); rabbit anti-HURP (for immunoblotting; Bethyl Labs, Montgomery, TX); goat anti-HURP (for immunofluorescence; Santa Cruz Biotechnology); mouse anti-Hec1 (9G3; AbCam, Cambridge, MA); and the human autoimmune serum CREST (ImmunoVision, Springdale, AR). Species-appropriate secondary antibodies conjugated to Alexa 488, Alexa 594, or Alexa 647 (for immunofluorescence) or to Alexa 700, Alexa 750, or Alexa 800 (for immunoblotting) were purchased from Invitrogen.

Immunoblotting

Lysates were prepared by washing cells three times with Dulbecco's PBS (DPBS), suspending them in 2× Laemmli buffer, and boiling them for 5 min. Mitotic lysates were prepared by synchronizing cells with a thymidine block; 10 h after thymidine washout, cells were arrested in mitosis for 3 h in 10 µM STLC; the plates were rinsed three times in DPBS; and mitotic cells were collected by shake-off, lysed in 2× Laemmli buffer, and boiled as described. Proteins were resolved by SDS–PAGE and transferred to nitrocellulose membranes. Membranes were blocked with Odyssey Blocking Buffer (LI-COR Biosciences, Lincoln, NE), probed with primary antibodies diluted in 5% (wt/vol) milk in PBS–Tween-20 (PBST) for 1 h, and then probed with species-appropriate fluorescently tagged secondary antibodies in PBST plus milk for 45 min. Fluorescence was measured with an Odyssey fluorescence detection system (LI-COR Biosciences).

Immunofluorescence and fixed-cell imaging

Cells subjected to nocodazole shock were permeabilized for 20 s at room temperature in PermFix (100 mM K 1,4-piperazinediethanesulfonic acid, pH 6.8, 0.2% Triton X-100, 10 mM K ethylene glycol tetraacetic acid, 1 mM $MgCl_2$) immediately before fixation. Cells subjected to cold were permeabilized for 1 min on ice in PermFix. All cells were fixed in methanol at –20°C for 10 min. Rinses were performed with Tris-buffered saline plus 0.1% Triton X-100 (TBST). Coverslips were blocked with AbDil (TBST + 2 mg/ml bovine serum albumin [Sigma-Aldrich]) for 10 min, probed with primary antibodies diluted in AbDil for 1 h, rinsed, probed with secondary antibodies diluted in AbDil for 45 min, and rinsed. DNA was stained with 5 µg/ml Hoechst 33342. Coverslips were mounted in Prolong Gold (Invitrogen).

Fixed cells were imaged using a 60×/1.4 numerical aperture (NA) objective (Olympus, Tokyo, Japan) with 1.6× auxiliary magnification on a DeltaVision Elite imaging system (Applied Precision, Issaquah, WA). Optical sections were collected every 0.2 nm. Ratio deconvolution and maximum-*Z* projection were performed in SoftWoRx (Applied Precision). Images were prepared for publication using ImageJ (National Institutes of Health, Bethesda, MD) and NIS-Elements (Nikon, Tokyo, Japan) software. All images are maximum-*Z* projections of deconvolved image stacks. Quantification of spindle intensity was performed in NIS-Elements: for a single, central *Z*-plane, the average fluorophore intensity of the nonspindle cytoplasm was subtracted from the average fluorophore intensity of the spindle.

Live-cell imaging

For imaging of spindle maintenance or collapse, cells were plated to MatTek dishes (MatTek, Ashland, MA). HeLa cells were transfected with mCherry-tubulin ~24 h after plating and imaged 48 h after plating. RPE-1/mCherry-tubulin stable cells were imaged 24–48 h after plating. Cells were imaged at 37°C with ~5% CO_2 using a 60×/1.4 NA objective (Olympus) on a DeltaVision Elite imaging system equipped with a WeatherStation environmental chamber (Applied Precision). At 100 min before imaging, culturing media was exchanged for 5 µM MG-132 in 1-ml movie medium (L-15 medium without phenol red supplemented with 10% FBS, antibiotics, and 7 mM K 4-(2-hydroxyethyl)-1-piperazineethanesulfonic acid, pH 7.7). Immediately before imaging, an additional 1 ml of movie medium with 5 µM MG-132 and 20 µM STLC was added. Several fields of view were chosen; for each field of view, five optical sections, 1.5 µm apart, were imaged every 90 s for 1 h. Maximum-*Z* projections are shown.

For imaging of mitotic timing, RPE-1 cells were plated to MatTek dishes and imaged 24 h after plating. Cells were imaged at 37°C with ~5% CO_2 using a 40×/1.3 NA objective (Olympus) on a DeltaVision Core imaging system equipped with a WeatherStation environmental chamber (Applied Precision). One hour before imaging, culturing media was exchanged for 2 ml of movie medium with or without 2.5 nM Taxol. Immediately before imaging, the dish lid was removed, and the medium was overlaid with mineral oil. Several fields of view were chosen; for each field of view, four optical sections, 2 µm apart, were imaged every 3 min for 5 h.

Statistical analysis

We performed *t* tests (two-tailed, assuming unequal variance) with the TTEST function in Excel (Microsoft, Redmond, WA).

ACKNOWLEDGMENTS

We thank James Orth, Susan Wente, Bob Coffey, and Dave Cortez for cell lines; Aaron Groen and Timothy Mitchison for anti-Eg5 antibody; and Linda Wordeman for insightful discussions. We thank members of the R. Ohi lab for critical reading of the manuscript. This work was supported by Vanderbilt University Medical Center Molecular Biophysics Training Grant T32 GM08320 to A.S.G. and National Institutes of Health Grant R01 GM086610 to R.O. R.O. is a Scholar of the Leukemia and Lymphoma Society.

REFERENCES

Bakhoum SF, Genovese G, Compton DA (2009). Deviant kinetochore microtubule dynamics underlie chromosomal instability. Curr Biol 19, 1937–1942.

Blangy A, Lane HA, d'Herin P, Harper M, Kress M, Nigg EA (1995). Phosphorylation by p34cdc2 regulates spindle association of human Eg5, a kinesin-related motor essential for bipolar spindle formation in vivo. Cell 83, 1159–1169.

Boleti H, Karsenti E, Vernos I (1996). Xklp2, a novel *Xenopus* centrosomal kinesin-like protein required for centrosome separation during mitosis. Cell 84, 49–59.

DeBonis S, Skoufias DA, Lebeau L, Lopez R, Robin G, Margolis RL, Wade RH, Kozielski F (2004). In vitro screening for inhibitors of the human mitotic kinesin Eg5 with antimitotic and antitumor activities. Mol Cancer Ther 3, 1079–1090.

DeLuca JG, Moree B, Hickey JM, Kilmartin JV, Salmon ED (2002). hNuf2 inhibition blocks stable kinetochore-microtubule attachment and induces mitotic cell death in HeLa cells. J Cell Biol 159, 549–555.

Dick AE, Gerlich DW (2013). Kinetic framework of spindle assembly checkpoint signalling. Nat Cell Biol 15, 1370–1377.

Dogterom M, Yurke B (1997). Measurement of the force-velocity relation for growing microtubules. Science 278, 856–860.

Felgner H, Frank R, Biernat J, Mandelkow EM, Mandelkow E, Ludin B, Matus A, Schliwa M (1997). Domains of neuronal microtubule-associated

proteins and flexural rigidity of microtubules. J Cell Biol 138, 1067–1075.
Ganem NJ, Compton DA (2004). The KinI kinesin Kif2a is required for bipolar spindle assembly through a functional relationship with MCAK. J Cell Biol 166, 473–478.
Goshima G, Wollman R, Stuurman N, Scholey JM, Vale RD (2005). Length control of the metaphase spindle. Curr Biol 15, 1979–1988.
Houghtaling BR, Yang G, Matov A, Danuser G, Kapoor TM (2009). Op18 reveals the contribution of nonkinetochore microtubules to the dynamic organization of the vertebrate meiotic spindle. Proc Natl Acad Sci USA 106, 15338–15343.
Kabeche L, Compton DA (2013). Cyclin A regulates kinetochore microtubules to promote faithful chromosome segregation. Nature 502, 110–113.
Kapitein LC, Peterman EJ, Kwok BH, Kim JH, Kapoor TM, Schmidt CF (2005). The bipolar mitotic kinesin Eg5 moves on both microtubules that it crosslinks. Nature 435, 114–118.
Kapoor TM, Mayer TU, Coughlin ML, Mitchison TJ (2000). Probing spindle assembly mechanisms with monastrol, a small molecule inhibitor of the mitotic kinesin, Eg5. J Cell Biol 150, 975–988.
Kollu S, Bakhoum SF, Compton DA (2009). Interplay of microtubule dynamics and sliding during bipolar spindle formation in mammalian cells. Curr Biol 19, 2108–2113.
Manning AL, Bakhoum SF, Maffini S, Correia-Melo C, Maiato H, Compton DA (2010). CLASP1, astrin and Kif2b form a molecular switch that regulates kinetochore-microtubule dynamics to promote mitotic progression and fidelity. EMBO J 29, 3531–3543.
McEwen BF, Heagle AB, Cassels GO, Buttle KF, Rieder CL (1997). Kinetochore fiber maturation in PtK1 cells and its implications for the mechanisms of chromosome congression and anaphase onset. J Cell Biol 137, 1567–1580.
Mitchison TJ, Maddox P, Gaetz J, Groen A, Shirasu M, Desai A, Salmon ED, Kapoor TM (2005). Roles of polymerization dynamics, opposed motors, and a tensile element in governing the length of *Xenopus* extract meiotic spindles. Mol Biol Cell 16, 3064–3076.
Miyamoto DT, Perlman ZE, Burbank KS, Groen AC, Mitchison TJ (2004). The kinesin Eg5 drives poleward microtubule flux in *Xenopus laevis* egg extract spindles. J Cell Biol 167, 813–818.
Sawin KE, LeGuellec K, Philippe M, Mitchison TJ (1992). Mitotic spindle organization by a plus-end-directed microtubule motor. Nature 359, 540–543.
Sharp DJ, Yu KR, Sisson JC, Sullivan W, Scholey JM (1999). Antagonistic microtubule-sliding motors position mitotic centrosomes in *Drosophila* early embryos. Nat Cell Biol 1, 51–54.
Sillje HH, Nagel S, Korner R, Nigg EA (2006). HURP is a Ran-importin beta-regulated protein that stabilizes kinetochore microtubules in the vicinity of chromosomes. Curr Biol 16, 731–742.
Sturgill EG, Ohi R (2013). Kinesin-12 differentially affects spindle assembly depending on its microtubule substrate. Curr Biol 23, 1280–1290.
Tanenbaum ME, Macurek L, Galjart N, Medema RH (2008). Dynein, Lis1 and CLIP-170 counteract Eg5-dependent centrosome separation during bipolar spindle assembly. EMBO J 27, 3235–3245.
Tanenbaum ME, Macurek L, Janssen A, Geers EF, Alvarez-Fernandez M, Medema RH (2009). Kif15 cooperates with eg5 to promote bipolar spindle assembly. Curr Biol 19, 1703–1711.
Tanenbaum ME, Medema RH (2010). Mechanisms of centrosome separation and bipolar spindle assembly. Dev Cell 19, 797–806.
Thein KH, Kleylein-Sohn J, Nigg EA, Gruneberg U (2007). Astrin is required for the maintenance of sister chromatid cohesion and centrosome integrity. J Cell Biol 178, 345–354.
Toso A, Winter JR, Garrod AJ, Amaro AC, Meraldi P, McAinsh AD (2009). Kinetochore-generated pushing forces separate centrosomes during bipolar spindle assembly. J Cell Biol 184, 365–372.
Uteng M, Hentrich C, Miura K, Bieling P, Surrey T (2008). Poleward transport of Eg5 by dynein-dynactin in *Xenopus laevis* egg extract spindles. J Cell Biol 182, 715–726.
Vanneste D, Takagi M, Imamoto N, Vernos I (2009). The role of Hklp2 in the stabilization and maintenance of spindle bipolarity. Curr Biol 19, 1712–1717.
Vladimirou E, McHedlishvili N, Gasic I, Armond JW, Samora CP, Meraldi P, McAinsh AD (2013). Nonautonomous movement of chromosomes in mitosis. Dev Cell 27, 60–71.
Ye F, Tan L, Yang Q, Xia Y, Deng LW, Murata-Hori M, Liou YC (2011). HURP regulates chromosome congression by modulating kinesin Kif18A function. Curr Biol 21, 1584–1591.
Yi Q, Zhao X, Huang Y, Ma T, Zhang Y, Hou H, Cooke HJ, Yang DQ, Wu M, Shi Q (2011). p53 dependent centrosome clustering prevents multipolar mitosis in tetraploid cells. PLoS One 6, e27304.
Zhai Y, Kronebusch PJ, Borisy GG (1995). Kinetochore microtubule dynamics and the metaphase-anaphase transition. J Cell Biol 131, 721–734.